

cDNA microarray study to identify expression changes relevant for apoptosis in K562 cells co-treated with amifostine and imatinib

Michele Bianchini · Giovanni Martinelli ·
Matteo Renzulli · Marcela Gonzalez Cid ·
Irene Larripa

Received: 17 January 2006 / Accepted: 29 May 2006 / Published online: 29 September 2006
© Springer-Verlag 2006

Abstract

Purpose Chronic myeloid leukemia is a clonal myeloproliferative disorder characterized by the presence of the fusion gene BCR/ABL. We had previously demonstrated an increased proapoptotic effect of imatinib (STI571) in combination with amifostine (AMI) in K562 cell line. In this study, we used genomic scale gene expression profiling to monitor changes at transcriptional level in K562 cells during the treatment with AMI + STI571.

Materials and methods cRNA from Control and treated K562 cells were mixed in equal amounts and incubated with a microarray slide for hybridization. RNA from six independent paired experiments was subjected to transcriptional profiling. With the aim to automate the process of biological theme determination, selected genes were further analyzed by EASE. Validation of the expression was carried out by quantitative real-time PCR and western blotting.

Results As expected, a small percentage of genes accounts for the effects of the combined drug treatment. We identified 61 sequences corresponding to known genes; 17 of the 61 genes were up regulated, such as RHO6, PPP2R5E, PPM1E and BTF that appear to reflect favorable events for apoptosis induction.

Between down regulated genes, API5, TUBB2 and TLK1 are also of considerable interest.

Conclusion We identified a transcriptional repressor of survival genes, known as BTF, which triggers a proapoptotic signal, potentially helpful to overcome the resistance to STI571. This finding could be particularly useful to design novel therapeutic strategies for leukemia patients. This study demonstrates the importance of in vitro testing of a novel drug combination most likely to predict its potential usefulness for in vivo application.

Keywords Microarray · Apoptosis · Amifostine · Imatinib · BTF

Introduction

Chronic myeloid leukemia (CML) is a clonal myeloproliferative disorder, arising from neoplastic transformation of hematopoietic stem cells [1]. Most of these cells are characterized by the presence of the Philadelphia (Ph) chromosome, a result of a cytogenetic translocation that is identified up to 95% of CML patients [2]. The Ph chromosome results in the formation of a fusion gene BCR/ABL that is a constitutively active tyrosine kinase (p210^{BCR/ABL}). Elevated kinase activity has been related with oncogenic signals in several systems, indeed the oncoprotein p210^{BCR/ABL} has been associated with growth factor independence and suppression of apoptosis, both strategies through which BCR/ABL induces oncogenic transformation [3, 4]. Programmed cell death, as well known, can be triggered by both mitochondrial (“intrinsic”) and death receptor (“extrinsic”) pathways, that represent two independent

M. Bianchini (✉) · M. Gonzalez Cid · I. Larripa
Departamento de Genética, Instituto de Investigaciones
Hematológicas “Mariano R. Castex”,
Academia Nacional de Medicina, Pacheco de Melo 3081,
1425 Capital Federal Buenos Aires, Argentina
e-mail: mbianchini@hematologia.anm.edu.ar

G. Martinelli · M. Renzulli
Institute of Hematology and Medical Oncology
“L. e A. Seragnoli”, University of Bologna, Bologna, Italy

pro-apoptotic mechanisms in most types of cells. The anti-apoptotic effect of BCR/ABL is exerted through interactions with various proteins that transduce the oncogenic signal responsible for the alteration of mitochondrial apoptosis [5]. Recently, molecules that specifically target the BCR/ABL gene product have been developed; one such molecule is the BCR/ABL inhibitor imatinib (GleevecTM or STI571, Novartis Pharma, Switzerland). Imatinib, a derivative of 2-phenylamino-pyrimidine, was originally thought to inhibit kinase activity by acting as a competitive inhibitor of the ATP-binding pocket. However, recent structural resolution of the ABL catalytic domain complexed with an imatinib homologue, showed that the drug occupies only part of the ATP-binding pocket of the enzyme, and that it produces its inhibitory effects by binding to and stabilizing the inactive, non-ATP binding form of BCR–ABL [6]. This compound has shown to be a potent antiproliferative and pro-apoptotic mediator [7]. Patients with CML treated with imatinib in early chronic phase tend to have durable remissions, but there is a high rate of relapse in patients with advanced disease [8]. At the time of relapse, patients typically show the reappearance of a fully active BCR/ABL protein. This observation has been confirmed by several but not all groups, since further BCR/ABL kinase independent pathways have been proposed [9, 10]. This would indicate that there are leukemia cells that overcome the pro-apoptotic effect of imatinib and survive in the presence of pharmacological concentrations of the drug [11]. Potential mechanisms of resistance to imatinib in Ph-positive leukemia are: (a) mutations in the BCR/ABL gene, predominantly in the kinase domain; (b) BCR/ABL gene amplification and increased BCR/ABL protein expression; (c) the switch to alternative kinase signaling pathways; (d) mechanisms related to pharmacokinetic factors of drug delivery [12]. For these reasons, many investigators are also examining the *in vitro* effect of imatinib when used in conjunction with other chemotherapeutic compounds [13–15]. In our laboratory, we had previously demonstrated the additive pro-apoptotic effect of imatinib when used in combination with the antioxidant agent amifostine (AMI; Actifos, Laboratorios Filaxis, Argentina) in K562 cell line [16]. The rationale for studying the potential additive effect of imatinib and AMI in the erythroblastic K562 cell line, derived from the interesting results published by Sattler and coworkers [17]; they showed that exogenous expression of p210^{BCR/ABL} in BA/F3, 32Dcl3 and M07e hematopoietic cell lines results in an increase of reactive oxygen species (ROS) in comparison with their untransformed counterparts. Consequently, we reasoned that drugs that would lower

ROS through supplementing the antioxidative potential of cells would be efficient in CML treatment, especially if used in combination with BCR/ABL kinase inhibitors such as imatinib. Our results showed that AMI in combination with imatinib at submicromolar concentrations has an additive effect in K562 cell line, while it does not have severe toxic effects in Ph chromosome negative cell lines such as U-937, HL60 and polymorphonuclear from peripheral blood from normal donors. Although the effects of AMI + STI571 on K562 cells have been studied *in vitro*, the molecular consequences of co-treatment have not been investigated. In this study, we used genomic scale gene expression profiling to monitor changes at transcription level in K562 cells during the treatment with AMI + STI571. Our main interest was to determine molecular alteration specifically due to simultaneous presence of the two agents. We show here that the combination of the two agents induced or repressed the expression of a limited set of genes, among them, we found several genes that provide insights helpful to understand the molecular mechanism underlying the observed additive effect on apoptosis. Furthermore, these insights could also help to design therapeutic strategies aimed at disrupting specific branches of BCR/ABL-induced oncogenic pathways, in an attempt to kill the CML cell.

Materials and methods

Cell culture and drug treatment

K562 cells were maintained in a 5% CO₂ atmosphere at 37°C in RPMI 1640 medium supplemented with 10% heat inactivated (30 min, 65°C) fetal bovine serum. Cells were used for the studies in passages 3–10 following thawing. For microarray study, K562 cells were treated during 48 h with: imatinib at 1 µM, AMI at 0.75 mg/ml and co-treated with AMI (0.75 mg/ml) added 15 min before imatinib (1 µM). On the other hand, for quantitative real-time confirmation study, K562 cells were incubated during 8, 24 and 48 h in the presence of imatinib (1 µM), AMI (0.75 mg/ml) or co-treated with AMI + STI571 as described above.

Fluorescence microscopy for apoptosis and viability assessment

Cell viability and apoptosis were assessed by fluorescence microscopy, following staining of cells with a mixture of acridine orange (100 mg/ml) and ethidium bromide (100 mg/ml) in phosphate buffered saline. One microliter of dye mix was placed in the bottom of

an eppendorf tube; 25 μ l of cell suspension (at 1×10^6 cells/ml) were added and mixed gently. Ten microliters of this mixture were placed on a clean microscope slide and at least 200 cells were examined with a 40 \times dry objective, using a suitable combination of filters. This methodology allows recognizing viable, apoptotic and necrotic cells.

RNA extraction amplification and labeling

Total RNA was extracted from K562 cultured cells using Trizol reagent (Invitrogen Life Technology Inc., Rockville, MD, USA) as recommended by the manufacturer. With the aim to reduce process variability in microarray results, cells were harvested and all RNAs were isolated immediately after 48 h of treatment, using reagents from the same lots and having a single responsible for all the bench manipulations. Prior to submission of samples for cDNA microarray analysis, cells from each assay were analyzed by fluorescence microscopy, to insure that a detectable drug effect had occurred at the morphological level, as judged by an increase in apoptotic cells. In order to assure that the gene expression measured by microarray assay was not affected by degradation of the RNA extracted from the cells, we used the Agilent 2100 Bioanalyzer (Agilent Technologies, Deutschland GmbH) to measure both the concentration and the quality/integrity of total RNA samples. Starting with 5 μ g of purified total RNA, double stranded cDNA was synthesized from full-length mRNA and subsequently transcribed in vitro using Amino Allyl MessageAmp II aRNA Amplification Kit (Ambion Europe Ltd. UK) to form amino allyl-cRNA. To exclude the presence of truncated cRNA transcripts and/or protein contamination 260/280 absorbance reading was obtained for cRNA; acceptable $A_{260/280}$ ratios fall in the range of 1.8 to 2.1 (in 10 mM Tris, 1 mM EDTA [pH 8]). Following labeling reaction with amine-modified forms of cyanine3 (Cy3) and cyanine5 (Cy5) dyes, and subsequently purification of fluorescent labeled probe we estimated quantity and size distribution of the labeled cRNA by agarose gel electrophoresis. Immediately after labeling, the two labeled cRNAs were separated from unincorporated nucleotides by filtration, mixed in equal proportions, and hybridized to SS-Human 19 Kv7 microarrays from University Health Network Microarray Centre (Ontario, CANADA) at 65°C overnight. After hybridization, each microarray was washed with 2 \times SSC, 0.03% SDS for 5 min at 65°C and then with 1 \times SSC for 5 min and 0.1 \times SSC for 5 min, both at room temperature.

Image acquisition and data analysis

SS-Human 19 Kv7 microarray contains 19,200 probes derived from coding and EST sequences deposited in GenBank. Arrays were scanned using an Affymetrix 428 scanner (MWG, Germany). Primary data collection and analysis were carried out using ImageScan Pro3.0 (MWG, Germany). Areas of the array with obvious blemishes were manually flagged and excluded from subsequent analyses. The raw data were deposited into Gene Expression Omnibus (GEO) repository (<http://www.ncbi.nlm.nih.gov/projects/geo/> accession: GSE3212). Fluorescence intensity data for each microarray were loaded on Microarray Data Analysis System (MIDAS) v2.18 software (from TIGR The Institute for Genomic Research), an application that allows the user to perform normalization and data analysis. Using MIDAS, we applied the following criteria: (1) Quality control flags for spots in each channel. (2) Channels background checking was applied taking in account a signal/noise ratio threshold = 2. (3) Iterative log-mean centering normalization function was applied to normalize channel intensities by applying a data range of 3 standard deviations. (4) Low intensity filter; threshold for Cy3 = 3,000 and Cy5 = 2,500. (5) Flip dye consistency checking function allows filtering out spots that show expression level inconsistency between a pair of flip-dye replicates; for this criterion we used a standard deviation filter.

Functional clustering and gene annotation were carried out by EASE (Expression Analysis Systematic Explorer) from National Institutes of Health; this is a powerful tool to automate the process of biological theme determination [18]. EASE rapidly converts a list of genes into an ordered table of robust biological themes that summarize the biological result of the microarray data. EASE calculates the Ease Score (ES) that is the default metric used by the software to rank categories of genes by over-representation.

Design for a 2 \times 2 factorial experiment

To identify a list of genes that best distinguishes the joint effect of the two drugs from what might be predicted on the basis of their effects alone, we decided to apply a class of experimental design named multifactorial design, as described by Yang and Speed [19]. If we let C denote mRNA that is derived from the untreated cells (Control), and A and S denote mRNA that is derived from the cells that were treated by AMI and imatinib separately, we can then use AS to denote cells that were treated with both drugs simultaneously. Since our main interest was to identify gene variations

due to the drug interaction (named “AS effect”), experimental design that offers the best precision (i.e., lowest variance), is a balance of direct and indirect comparison (see hybridization design in Fig. 1).

To measure the extent to which relative expression levels of genes differ for the effect of the two agents we applied the following calculation:

$$\text{Log}_2(\text{AS}/\text{A}) - \text{Log}_2(\text{AS} \times \text{C}/\text{A} \times \text{S}) \rightarrow \delta.$$

Following this formula, “AS effect” (i.e., fold change) is then defined as: $\pm 2^{|\delta|}$, where $|\delta|$ is the absolute value of the difference in \log_2 scale between $[\text{AMI} + \text{STI}_{(\text{signal})}/\text{AMI}_{(\text{signal})}]$ and $[\text{STI}_{(\text{signal})}/\text{Control}_{(\text{signal})}]$.

The positive sign (+) indicates up-regulation in co-treated cells compared to control, while the negative sign (−) indicates down-regulation. Note that a fold change of 1.0 is equivalent to no difference in gene expression. Differences between groups were assessed using paired *t* test ($P < 0.01$).

Real-time PCR

cDNAs were synthesized from RNA samples extracted from new treatments (biological replicates) carried out as described for microarray experiment. DNA was digested with RNase-free DNase I for 30 min at 37°C using a DNA-free™ kit (Ambion Inc., USA); following digestion, DNase was then inactivated and removed using DNase inactivation reagent included in the kit. Reverse transcription was performed on 1 µg of total RNA for 50 min at 42°C using an oligo(dT) primer and Superscript II reverse transcriptase (Invitrogen Life Technology Inc., Rockville, MD, USA). RT-PCR products were analyzed in triple determinations, for the expression of two target genes (RHO6 and BTF) by quantitative real-time PCR (qRT-PCR). To control for variations in amounts of RNA, GAPDH and

β -actin were also tested as housekeeping genes. All PCR reactions were performed in a LightCycler® 2.0 instrument using the LC-FastStart DNA Master SYBR Green I Kit (Roche Diagnostics, Mannheim, Germany). The primer sequences used in this study, amplicon sizes, annealing temperatures and primers concentrations are given in Table 1. Thermocycling for each reaction was performed in a final volume of 20 µl containing 2 µl cDNA sample, 4 mmol/l MgCl₂, 0.5 µmol/l of each primer and 2 µl LC-FastStart DNA Master SYBR Green. After 10 min of initial denaturation at 95°C, the cycling conditions consisted of denaturation at 95°C for 6 s, annealing for 10 s (see temperatures in Table 1) and elongation at 72°C for 6 s. After amplification, the temperature was slowly raised above the melting point of the PCR product to measure the fluorescence for the melting curve (this enables the identification of specific transcripts). Calibration curves were prepared by amplification of each gene (targets and housekeeping) from serial dilutions of cDNA obtained from the K562 cell line; we independently do multiple serial dilution curves to determine an average efficiency to plug that value into the formula. Resulting efficiencies of the amplicons were not sufficient equal, this means that PCRs do not perform equally efficiently. For this reason, Pfaffl method was used to evaluate the real-time PCR data [20]. Expression levels of target genes were expressed relative to the expression levels of GAPDH and β -Actin (reference genes). For each run, an average PCR threshold cycle (Cp) value for the genes was determined as the mean of triplicate determinations (AVECp). The calculations for the quantification start with getting the difference (ΔCp) between the AVECp values of the treated [AVECp (treated)] and the control or untreated cells [AVECp (control)] for each pair of primers (ΔCp_n):

$$\Delta\text{Cp}_n = \text{AVECp}(\text{treated}) - \text{AVECp}(\text{control}).$$

This value is calculated for each sample to be quantified; K562 untreated sample was chosen as the baseline for each comparison to be made. The Pfaffl calculation involves finding the ratio between each target's ΔCp and the reference's ΔCp , taking in account different efficiency value. The formula for this is:

$$\text{Ratio} = \frac{(E)^{\Delta\text{Cp}_{\text{target}}}}{(E)^{\Delta\text{Cp}_{\text{ref}}}}.$$

All PCR products were checked by melting point analysis and by gel electrophoresis to verify that products were of the correct size (see Figs. 2, 3).

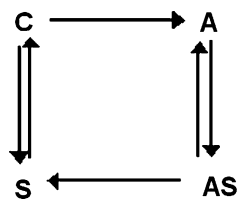


Fig. 1 Schematic representation of the experimental design. In this representation C, A, S and AS correspond to target mRNA samples and arrows correspond to hybridizations (i.e., microarray slides) between two mRNA samples. C untreated cells mRNA, A amifostine treated cells mRNA, S imatinib treated cells mRNA, AS amifostine + imatinib treated cells mRNA. Dye swap replication has been carried out between C–S and A–AS

Table 1 Primer sequences, amplicon's length and primer concentrations for Btf, Rho6, GAPDH, Actin- β and BCR/ABL genes confirmed with quantitative real-time PCR

Transcript	GenBank	Product size (bp)	Primer concentration (nmol/l)	Sequence
Btf/Bclaf1	NM_014739	141	200	5'-CCTTCACCTATTGCTACACCAC-3'
			200	5'-ACCAGACCCAGACCTTTTCAG-3'
Rho6/RND1	NM_014470	75	200	5'-ACAGAGGAACAGAGGGTGG-3'
			200	5'-GAGTGGACGGACATTATCGTAG-3'
BCR/ABL	HSA131466	150	300	5'-TCCGC TGACCATCAATAAGGA-3'
			300	5'-TT GAGCCTCAGGGTCTGAGTG-3'
Actin- β	NM_001101	103	200	5'-CACTCTTCCAGCCTTCCTTC-3'
			200	5'-TACAGGTCTTTGCGGATGTC-3'
GAPDH	NM_002046	117	200	5'-TCAAGAAGGTGGTGAAGCAG-3'
			200	5'-CGTCAAAGGTGGAGGAGTG-3'

Western blot analysis

K562 cells were washed twice in PBS, then lysed in 0.2 ml of lysis buffer (50 mM Tris-HCl pH 8, 150 mM NaCl, 0.1% SDS, 0.5% DCS, 1% NP-40, 5 mM EDTA) containing a protease inhibitor cocktail for mammalian tissues (SIGMA, MO, USA). After 30 min on ice, they were homogenized by ten passages through a 25-gauge needle, and centrifuged in a microfuge (9,300 g) for 10 min at 4°C. An aliquot of the supernatant was saved for protein quantification by Bradford method. Supernatants were mixed with 4× electrophoresis sample buffer, separated by sodium dodecylsulphatepolyacrylamide gel electrophoresis (SDS-PAGE), and then the proteins were transferred to nitrocellulose sheets. Membranes were saturated in PBS containing 5% non-fat dry milk (blocking buffer) for 60 min, then incubated for 1 h in blocking buffer containing the primary antibody specific for BTF (clone 5; BD Biosciences Pharmingen, USA). After four washes in PBS containing 0.1% Tween-20, they were incubated for 45 min at room temperature with the secondary antibody (goat anti-mouse alkaline phosphatase), diluted 1:5,000 in blocking buffer, and washed as above. Signals were detected using BCIP/NBT color development substrate (Promega, Madison, USA). All blots were also probed with anti-GAPDH (BD Transduction Laboratories, USA) monoclonal antibody to ensure equal loading.

Results

In this study, we used genomic-scale gene expression profiling to monitor changes at transcriptional level in K562 cells, treated with two chemical agents: imatinib, a selective ABL family tyrosine kinases inhibitor and

AMI, an aminothioliol compound dephosphorylated at the tissue site by alkaline phosphatase. Following total RNA extraction, cRNA is obtained by in vitro transcription of dsDNA, from both the test and the control samples in the presence of amino allyl UTP that are finally labeled with different fluorochromes. Test and control cRNA samples are mixed in equal amounts and incubated with cDNA microarrays for hybridization. This hybridization method, known as dual-color system, allows assessment of expression in the test sample in relation to expression in the control sample; moreover, for two microarrays we used a dye-swap replicate approach that enabled us to correct for dye-bias resulting from differences in efficiencies of dye incorporation. RNA from six independent experiments was subjected to transcriptional profiling following the experimental design described in [Materials and methods](#) (Fig. 1). A measurable change (that we named “AS effect”, see [Materials and methods](#) for mathematical details) in expression between the control and treated cells was found in 12,796 (67%) of the total 19,200 sequences. From this gene data set, we selected only those genes that had statistically significant expression change (127 sequences, $P < 0.01$ Bonferroni Correction): 43 genes showed a “positive AS effect” (i.e., they are up regulated as consequence of the drug-joint effect) while for 84 genes we reported a “negative AS effect” (i.e., they are down regulated as consequence of the drug-joint effect). However, only 61 of the 127 sequences corresponded to known genes; although the changes in gene expression were found to be statistically significant, the relative fold change caused by AMI + STI571 were fairly modest for the vast majority of these sequences (Table 2). With the purpose to enable other users to comprehensively interpret and evaluate our results, complete tables of

Table 2 Differentially expressed genes between co-treated and untreated K562 cells

Gene symbol	Gene name	^a Positive AS effect
<i>RHO6</i>	GTP-binding protein	2.09
<i>PPM1E</i>	Protein phosphatase 1E (PP2C domain containing)	2.01
<i>LRIG2</i>	Leucine-rich repeats and immunoglobulin-like domains 2	1.84
<i>PPP2R5E</i>	Protein phosphatase 2, regulatory subunit B (B56), epsilon isoform	1.83
<i>CDKL3</i>	Cyclin-dependent kinase-like 3	1.81
<i>BCLP</i>	CAC-1	1.80
<i>Arhgef7</i>	Rho guanine nucleotide exchange factor (GEF) 7	1.80
<i>PEN2</i>	Presenilin enhancer 2	1.80
<i>DOM3Z</i>	Dom-3 homolog Z (<i>C. elegans</i>)	1.79
<i>BTF</i>	Bcl-2-associated transcription factor	1.78
<i>ZNF317</i>	Zinc finger protein 317	1.78
<i>FUT4</i>	Fucosyltransferase 4 (alpha (1,3) fucosyltransferase, myeloid-specific)	1.76
<i>CLCN6</i>	Chloride channel 6	1.75
<i>CSE-C</i>	Cytosolic sialic acid 9-O-acetylesterase homolog	1.73
<i>CELSR2</i>	Cadherin, EGF LAG seven-pass G-type receptor 2	1.73
<i>RNF24</i>	Ring finger protein 24	1.73
<i>FYB</i>	FYN binding protein (FYB-120/130)	1.72
Gene symbol	Gene name	^b Negative AS effect
<i>TUBB2</i>	Tubulin, beta, 2	– 2.41
<i>DC6</i>	DC6 protein	– 2.28
<i>DDR1</i>	Discoidin domain receptor family, member 1	– 2.15
<i>TIMELESS</i>	Timeless homolog (<i>Drosophila</i>)	– 2.08
<i>IKBKAP</i>	Inhibitor of kappa light polypeptide gene enhancer in B-cells	– 2.07
<i>HT002</i>	Hypertension-related calcium-regulated gene	– 2.06
<i>ASMTL</i>	Acetylserotonin O-methyltransferase-like	– 2.05
<i>NVL</i>	Nuclear VCP-like	– 1.99
<i>TLK1</i>	Tousled-like kinase 1	– 1.99
<i>LOC51064</i>	Glutathione S-transferase subunit 13 homolog	– 1.99
<i>CGI-121</i>	CGI-121 protein	– 1.95
<i>TIMP2</i>	Tissue inhibitor of metalloproteinase 2	– 1.93
<i>ECHS1</i>	Enoyl coenzyme A hydratase, short chain, 1, mitochondrial	– 1.91
<i>DPYSL5</i>	Dihydropyrimidinase-like 5	– 1.90
<i>STOM</i>	Stomatin	– 1.87
<i>PSMD10</i>	Proteasome (prosome, macropain) 26S subunit, non-ATPase	– 1.87
<i>SERPINE1</i>	Serine (or cysteine) proteinase inhibitor	– 1.86
<i>BLMH</i>	Bleomycin hydrolase	– 1.83
<i>NDUFS8</i>	NADH dehydrogenase (ubiquinone) Fe-S protein 8, 23kDa	– 1.83
<i>LDB2</i>	LIM domain binding 2	– 1.83
<i>GPR51</i>	G protein-coupled receptor 51	– 1.83
<i>UACA</i>	Uveal autoantigen with coiled-coil domains and ankyrin repeats	– 1.83
<i>RNF19</i>	Ring finger protein 19	– 1.83
<i>AZGP1</i>	Alpha-2-glycoprotein 1, zinc	– 1.82
<i>RXRA</i>	Retinoid X receptor, alpha	– 1.81
<i>GLMN</i>	FKBP-associated protein	– 1.81
<i>SKP2</i>	S-phase kinase-associated protein 2 (p45)	– 1.80
<i>GCC1</i>	Golgi coiled-coil 1	– 1.80
<i>PHGDH</i>	Phosphoglycerate dehydrogenase	– 1.79
<i>PACSN2</i>	Protein kinase C and casein kinase substrate in neurons 2	– 1.79
<i>CGI-128</i>	CGI-128 protein	– 1.77
<i>ODAG</i>	Ocular development-associated gene	– 1.77
<i>LOC144233</i>	Hypothetical protein LOC144233	– 1.76
<i>API5</i>	Apoptosis inhibitor 5	– 1.75
<i>SZF1</i>	KRAB-zinc finger protein SZF1-1	– 1.75
<i>ASPIN</i>	Asporin (LRR class 1)	– 1.74
<i>TUBB</i>	Tubulin, beta polypeptide	– 1.74
<i>VMP1</i>	Likely ortholog of rat vacuole membrane protein 1	– 1.73

Table 2 continued

	Gene symbol	Gene name	^b Negative AS effect
^a Up-regulated genes in treated cells (positive AS effect)	<i>ILF3</i>	Interleukin enhancer binding factor 3, 90kDa	– 1.73
	<i>SSPN</i>	Sarcospan (Kras oncogene-associated gene)	– 1.73
	<i>C14orf75</i>	Chromosome 14 open reading frame 75	– 1.72
^b Down-regulated genes in treated cells (negative AS effect)	<i>PLCB4</i>	Phospholipase C, beta 4	– 1.72
	<i>MGC3207</i>	Hypothetical protein MGC3207	– 1.72
	<i>MT2A</i>	Metallothionein 2A	– 1.71

original microarray data have been uploaded to the GEO repository (see the GEO website at <http://www.ncbi.nlm.nih.gov/projects/geo/accession:GSE3212>).

Microarray expression data from single treatments [i.e., $AMI_{(signal)}$ vs. $Control_{(signal)}$ and $STI571_{(signal)}$ vs. $Control_{(signal)}$] were also analyzed confirming that expression alteration observed for selected genes was mainly due to “AS effect” (data not shown). With the objective to automate the process of biological theme determination, in particular to discover those elements with apoptotic role, selected genes were further analyzed by EASE. Between significant up-regulated genes RHO6 (GTP-binding protein), PPP2R5E (protein phosphatase 2, regulatory subunit B), PPM1E (protein phosphatase 1E) and BTF (Bcl-2-associated transcription factor) appear to reflect favorable events for apoptosis induction (for details, see Table 3). Genes that resulted down regulated were also of considerable interest, e.g., TUBB2 (tubulin, beta, 2),

TLK1 (tousled-like kinase 1) and API5 (apoptosis inhibitor 5) (for details, see Table 4).

Validation studies

The qRT-PCR was used to confirm the reliability of the microarray results. We chose two sequences found to be up regulated as consequence of the “AS effect” at microarray analysis (BTF and RHO6) (Fig. 2). The qRT-PCR clearly confirmed the up-regulation of both genes in the treated sample relatively to untreated cells, supporting the microarray results (Fig. 3); moreover, since the quantitative confirmation study was carried out across three different time points (8, 24 and 40 h), we could observe that “AS effect” onto Btf expression increased in a time-dependent manner (Fig. 4). These data verified the reliability and rationality of our strategy to identify genes that are altered as a consequence of the treatment.

Table 3 Up-regulated proapoptotic genes

Gene symbol	Chromosome	Gene name	AS effect
RHO6	12q12-q13	GTP-binding protein	2.09
PPM1E	17q23.2	Protein phosphatase 1E (PP2C domain containing)	2.01
PPP2R5E	14q23.1	Protein phosphatase 2, regulatory subunit B (B56), epsilon isoform	1.83
Arhgef7	13q34	Rho guanine nucleotide exchange factor (GEF) 7	1.80
BTF	6q22-q23	Bcl-2-associated transcription factor	1.78
DAXX	6p21.3	Death associated protein 6	1.59
DAP3	1q21-q22	Death-associated protein-3	1.51
BFAR	16p13.13	Bifunctional apoptosis regulator	1.45

Table 4 Down-regulated antiapoptotic genes

Gene symbol	Chromosome	Gene name	AS effect
TUBB2		Tubulin, beta, 2	– 2.41
TLK1	2q31.1	Tousled-like kinase 1	– 1.99
GLMN	1p22.1	FKBP-associated protein	– 1.81
PACSIN2	22q13.2-13.33	Protein kinase C and casein kinase substrate in neurons 2	– 1.79
API5	11p12-q12	Apoptosis inhibitor 5	– 1.75

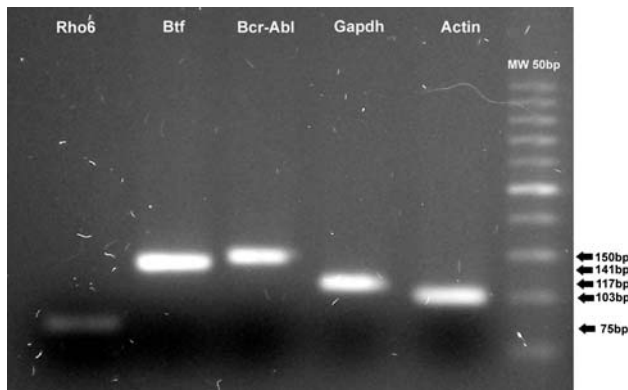


Fig. 2 Reverse transcriptase–polymerase chain reaction transcript analysis of Rho6, Btf, BCR/ABL, GAPDH and Actin- β . PCR primers were designed using the Primer3 software and synthesized by Invitrogen (Life Technologies). Primer sequences are given in Table 1. Conventional PCR to amplify the transcripts of interest was carried out using K562 cDNA. The reaction conditions were: 95° for 5 min, 35 cycles at 95° for 30 s, 60° for 30 s, 72° for 30 s followed by an extension phase of 5 min at 72°. The PCR products were separated on 3% agarose gel and stained with 10 μ l ethidium bromide prior to examination and photographing under UV light

BTF was chosen for protein expression validation because its increment may be useful to rescue the apoptotic phenotype in co-treated K562 cells. Using a commercial monoclonal antibody, we used western blotting analysis to compare BTF protein expression in treated versus untreated K562 (Fig. 5). Protein production for treated samples was consistent with mRNA levels measured by microarray and real-time PCR.

Discussion

As previously reported by us, an additive apoptotic effect of imatinib with the cytoprotective agent AMI in K562 cell line was observed in our laboratory after 72 h of treatment [16]. In the present study, using cDNA microarray technology, we investigated the molecular mechanism underlying the observed pro-apoptotic “AS effect” in K562 cells. The design for microarray experiment (named “2 \times 2 multifactorial design”) has been chosen with the objective to obtain the more reliable data to describe this joint effect [19]. When the biological effect of AMI + STI571 treatment was analyzed at molecular level, it was found that only few transcripts were significantly induced or reduced. Among these up- or down regulated genes, using EASE annotation tool, we were able to select those genes that can be related to apoptosis process; moreover, with the purpose to better characterize their molecular function we began to review PubMed bibliography.

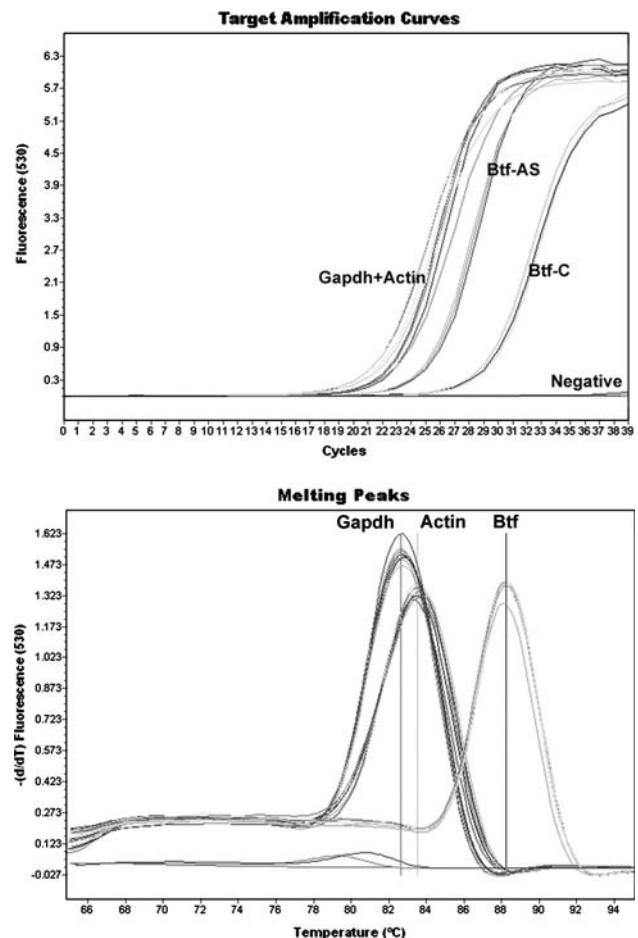
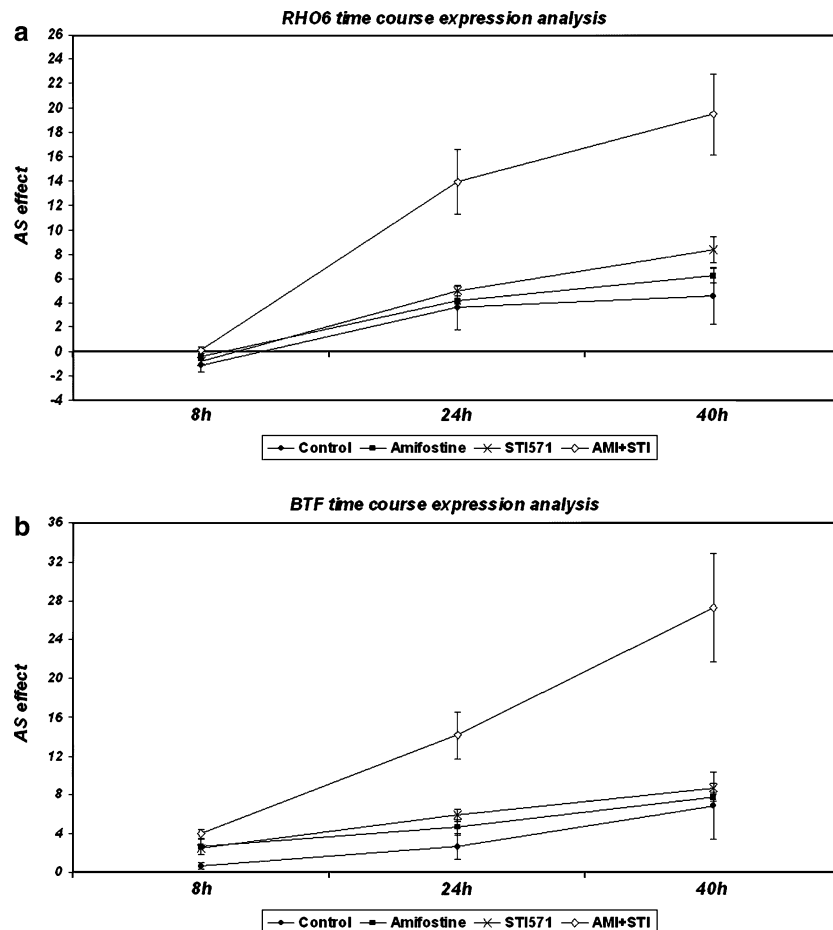


Fig. 3 Example of real-time PCR showing plots of the fluorescent signals versus cycle number (*top panel*) and melting curves (*bottom panel*). We employed the LightCycler 2.0 instrument to quantify the level of each transcript. All cDNA samples were simultaneously examined along with appropriate set of positive and negative controls. Primer sets used in this technique are given in Table 1. In the example, amplification curves (*top panel*) for BTF, GAPDH and Actin β were obtained from cDNAs synthesized using RNAs extracted from: K562 treated cells (BTF-AS and GAPDH-Actin) and K562 untreated cells (BTF-C and GAPDH-Actin). Average C_p values for each curve were used to determine BTF/GAPDH-Actin β ratios as described under **Materials and methods**. As negative control, a sample containing all reagents except cDNA was used in every PCR run; no reaction was noted in the negative control. Melting curve analysis (*bottom panel*) was used to determine the presence of non-specific amplification products. Melting assay ended all the analyses: samples were heated to 95°C (20°C/s) without hold, cooled to 55°C (20°C/s) hold for 15 s and then heated slowly at 0.1°C/s up to 95°C, finally cooled to 40°C (20°C/s). It is shown that the melting temperatures of the PCR products clustered in three major groups. These different melting points were in agreement with variation in the amplicon length for BTF, GAPDH and Actin β

Between down-regulated genes, we found a group mainly involved in microtubule organization, such as GLMN, PACSIN2, TLK1 and TUBB. It is well known that programmed cell death depends in part on

Fig. 4 Alteration (AS effect) in two transcripts in response to amifostine and/or imatinib as measured by qRT-PCR.

a, b The expression, as a function of time of treatment, of sequences classified as proapoptotic genes (RHO6 and BTF, respectively) that are significantly induced by amifostine and imatinib; the legends in **(a)** and **(b)** present the kind of each treatment, linked to the symbol used in the figure. AS effect values are mean of three experiments normalized as indicated in [Materials and methods](#)



microtubule network mobility; indeed, microtubules serve as scaffolds for signaling molecules, such as BIM and Survivin, whose release from microtubules affects the activities of these apoptotic regulators [21]. In addition, we found a gene, BLMH (Bleomycin Hydrolase), whose mRNA level was significantly lower in K562-treated cells than in K562-untreated cells. This finding strongly suggests that a novel combination of

AMI + STI571 with Bleomycin could be effective, since Bleomycin inactivation has been recognized as one mechanism of tumor resistance to this compound [22]. Additional studies are required to investigate this interesting possibility; clarification of whether similar abnormalities are involved in the imatinib resistance in primary cells from imatinib resistant leukemia patients is important, and such studies are now being carried

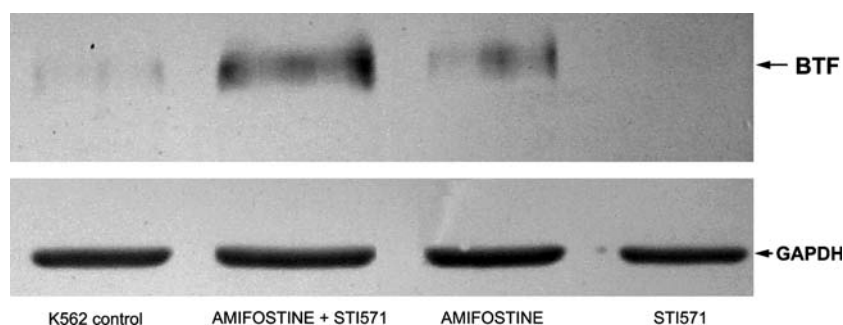


Fig. 5 Effect of amifostine and imatinib on BTF protein expression in K562 cells. Western blot analysis for BTF and GAPDH (protein loading control) was performed by using an alkaline phosphatase/BCIP-NBT color development system.

K562 cells were incubated for 40 h in the presence of amifostine, imatinib and a combination of both. Total cell lysates were prepared and separated by SDS-PAGE on 12% gels (5 µg protein/lane)

out in our laboratory. Importantly, expression profiling facilitated the novel discovery that AMI + STI571 treatment caused down-regulation of a gene described previously as being capable of hydrolyzing the amide bond of bleomycin, a glycopeptide that is clinically used as a chemotherapeutic agent in the treatment of human malignancies.

Noteworthy, between up-regulated genes due to “AS effect”, we found several serine/threonine protein phosphatases, such as PPM1E (member of the PP2C family) and PPP2R5E (regulatory subunits of PP2A family). The importance of phosphorylation and dephosphorylation in intracellular signaling pathways has long been recognized [23], although attention has focused mainly on kinases. Interestingly, recent reports suggest that the interaction of the serine/threonine protein phosphatase 1 (PP1) and protein phosphatase 2A (PP2A) with certain regulators of the Bcl-2 family is critically involved in the control of apoptosis. Such studies show how these phosphatases, that activate pro-apoptotic (BAD, BID, BIC) and inhibit anti-apoptotic [BCL-2, BCL-x(L)] proteins of the Bcl-2 family, can be considered molecules with a positive regulatory function in apoptosis [24, 25]. More recently, a direct suppression of PP2A activity by BCR/ABL expression has been demonstrated by Neviani and coworkers [26]. Altogether, these data suggest that pharmacological enhancement of PP2A activity represents a possible therapeutic strategy for blast crisis and imatinib resistant CML. However, it is conceivable that other protein phosphatases may contribute to the anti-oncogenic effect against BCR/ABL transformation in CML; identification of such genes cooperating with PP2A to the observed reduction in PTPase activity, will be important to understand the survival and proliferative function of BCR/ABL in hematopoietic cells. Here, we report that in response to AMI + STI571, there is a significant increment in transcription level for PP2A and PPM1E; functional studies to validate the role for PPM1E are in course in our laboratory.

Among the numerous genes examined in this study, we were able to determine at least two, RHO6 [27] and BTF [28], which have reported biologic significance in the context of apoptosis. RHO proteins are a branch of GTPases that belong to the RAS superfamily, which are critical elements of signal transduction pathways leading to a variety of cellular responses. This family of small GTPases has been involved in diverse biological functions such as cytoskeleton organization, cell growth and motility [29]. Moreover, as reported by Esteve et al. [30] several human RHO proteins are capable of inducing apoptosis in different cell systems

such as NIH3T3 and K562 cell lines. Consistent with this work, we can speculate that RHO6 over expression is partially responsible for the apoptotic phenotype observed in our system. In a subsequent publication, the same group demonstrated that RHO-dependent apoptosis is independent of p53 but it is mediated by the generation of ceramides [31]. This potential alternative apoptotic mechanism make sense for K562 cells since it is a p53-defective cell line, therefore additive pro-apoptotic effects must be necessarily determined through an alternative pathway independent from p53.

A second intriguingly gene was BTF (BCL-2-associated transcription factor) which interacts with the antiapoptotic family members BCL-2 and BCL-x(L) that, as described by Kasof et al. [28], sequester BTF in the cytoplasm and block its transcriptional repression activity onto survival genes. They also demonstrated that through BTF over expression, an alternatively apoptotic pathway was induced in a p53-deficient cell system. Thus, BTF may represent a novel tumor suppressor gene residing in a unique pathway by which the Bcl-2 family can regulate apoptosis. Similarly, we believe that the BTF over expression observed in our system could provide an alternative apoptotic pathway by which co-treated K562 cells are induced to programmed cell death. Therefore, future experiments, including DNA regulation profiling (i.e., ChIP-chip) in vitro after treatment of K562 cells with AMI + STI571 are now underway to examine the potential influence of BTF on the expression of genes in the “pro-apoptotic” cluster that we have identified.

In conclusion, the expression analysis by cDNA microarray revealed us a relatively new transcriptional repressor, known as BTF, which would trigger a pro-apoptotic signal, through which imatinib-resistant leukemic cells can partly restore apoptosis sensitivity. BTF binds to “antideath” BCL-2-related proteins such as, BCL-2 and BCL-x(L), through its C-terminal region, and this binding is thought to promote apoptosis by blocking their “antideath” activity. Changes in the redox state caused by AMI can overcome resistance to imatinib via induction of BTF-mediated gene expression; antioxidant activity could promote the translocation of Btf from the cytoplasm to the nucleus. It is well known that one mechanism of imatinib resistance in CML is due to BCR/ABL amplification; K562 cell line represents an in vitro model that reproduces this kind of drug resistance. Ideally, patients unlikely to respond to imatinib alone may benefit by combining imatinib with novel or conventional drugs [32]. These findings could be useful to better design novel therapeutic strategies with the aim to restore apoptosis sensitivity in CML patients with BCR/ABL gene

amplification [33, 34]. The data presented here creates an interesting rationale to further investigate STI571 and AMI as a potential therapeutic strategy in Ph-positive human leukemias with chimeric gene amplification and eventually p53-mutation.

Acknowledgments This paper was supported by grants from CONICET (Consejo Nacional de Investigaciones Científicas y Técnicas), ANPCyT (Agencia Nacional de Promoción Científica y Técnica), Academia Nacional de Medicina, Cofin 2003 (M. Baccarani), AIL, AIRC, Fondazione Del Monte di Bologna e Ravenna, FIRB 2001 and Ateneo 60% grants.

References

- Cortes JE, Talpaz M, Kantarjian H (1996) Chronic myelogenous leukemia: a review. *Am J Med* 100:555–570
- Laurent E, Talpaz M, Kantarjian H, Kurzrock R (2001) The BCR gene and Philadelphia chromosome-positive leukemogenesis. *Cancer Res* 61:2343–2355
- Faderl S, Talpaz M, Estrov Z, O'Brien S, Kurzrock R, Kantarjian HM (1999) The biology of chronic myeloid leukemia. *N Engl J Med* 341:164–172
- Evans C, Owen-Lynch P, Whetton AD, Dive C (1993) Activation of the Abelson tyrosine kinase activity is associated with suppression of apoptosis in hemopoietic cells. *Cancer Res* 53:1735–1738
- Goldman JM, Melo JV (2003) Chronic myeloid leukemia—advances in biology and new approaches to treatment. *N Engl J Med* 349:1451–1464
- Schindler T, Bornmann W, Pellicena P, Miller WT, Clarkson B, Kuriyan J (2000) Structural mechanism for STI-571 inhibition of abelson tyrosine kinase. *Science* 289:1938–1942
- Druker BJ, Sawyers CL, Kantarjian H, Resta DJ, Reese SF, Ford JM, Capdeville R, Talpaz M (2001) Activity of a specific inhibitor of the BCR/ABL tyrosine kinase in the blast crisis of chronic myeloid leukemia and acute lymphoblastic leukemia with the Philadelphia chromosome. *N Engl J Med* 344:1038–1042
- Deininger M, Buchdunger E, Druker BJ (2005a) The development of imatinib as a therapeutic agent for chronic myeloid leukemia. *Blood* 105(7):2640–2653
- Hochhaus A, Kreil S, Corbin AS, La Rosee P, Muller MC, Lahaye T, Hanfstein B, Schoch C, Cross NC, Berger U, Gschaidmeier H, Druker BJ, Hehlmann R (2002) Molecular and chromosomal mechanisms of resistance to imatinib (STI571) therapy. *Leukemia* 16(11):2190–2196
- Hui CH, Hughes TP (2003) Strategies for the treatment of imatinib-resistant chronic myeloid leukemia. *Clin Adv Hematol Oncol* 1(9):538–545, 559
- Mahon FX, Deininger MW, Schultheis B, Chabrol J, Reiffers J, Goldman JM, Melo JV (2000) Selection and characterization of BCR-ABL positive cell lines with differential sensitivity to the tyrosine kinase inhibitor STI571: diverse mechanisms of resistance. *Blood* 96:1070–1079
- Gambacorti-Passerini CB, Gunby RH, Piazza R, Galiotta A, Rostagno R, Scapozza L (2003) Molecular mechanisms of resistance to imatinib in Philadelphia-chromosome-positive leukaemias. *Lancet Oncol* 4(2):75–85
- Porosnicu M, Nimmanapalli R, Nguyen D, Worthington E, Perkins C, Bhalla KN (2001) Co-treatment with As₂O₃ enhances selective cytotoxic effects of STI-571 against Bcr-Abl-positive acute leukemia cells. *Leukemia* 5:772–778
- Kim JS, Jeung HK, Cheong JW, Maeng H, Lee ST, Hahn JS, Ko YW, Min YH (2004) Apicidin potentiates the imatinib-induced apoptosis of Bcr-Abl-positive human leukaemia cells by enhancing the activation of mitochondria-dependent caspase cascades. *Br J Haematol* 124(2):166–178
- Deininger M, Buchdunger E, Druker BJ (2005b) The development of imatinib as a therapeutic agent for chronic myeloid leukemia. *Blood* 105(7):2640–2653
- Vellon L, Gonzalez Cid M, Nebel MD, Larripa I (2005) Additive apoptotic effect of STI571 with the cytoprotective agent amifostine in K-562 cell line. *Cancer Chemother Pharmacol* 55:602–608
- Sattler M, Verma S, Shrikhande G, Byrne CH, Pride YB, Winkler T, Greenfield EA, Salgia R, Griffin JD (2000) The BCR/ABL tyrosine kinase induces production of reactive oxygen species in hematopoietic cells. *J Biol Chem* 275(32):24273–24278
- Hosack DA, Dennis G Jr, Sherman BT, Lane HC, Lempicki RA (2003) Identifying biological themes within lists of genes with EASE. *Genome Biol* 4(10):R70
- Yang YH, Speed T (2002) Design issues for cDNA microarray experiments. *Nat Rev Genet* 3:579–588
- Tichopad A, Dilger M, Schwarz G, Pfaffl MW (2003) Standardized determination of real-time PCR efficiency from a single reaction set-up. *Nucleic Acids Res* 31(22):6688
- Grzanka A, Grzanka D, Orlikowska M (2003) Cytoskeletal reorganization during process of apoptosis induced by cytostatic drugs in K-562 and HL-60 leukemia cell lines. *Biochem Pharmacol* 66(8):1611–1617
- Ferrando AA, Penda AM, Llano E, Velasco G, Lidereau R, Carlos Lopez-Otin C (1997) Gene characterization, promoter analysis, and chromosomal localization of human bleomycin hydrolase. *J Biol Chem* 272(52):33298–33304
- McCright B, Virshup DM (1995) Identification of a new family of protein phosphatase 2A regulatory subunits. *J Biol Chem* 270(44):26123–26128
- Klumpp S, Krieglstein J (2002) Serine/threonine protein phosphatases in apoptosis. *Curr Opin Pharmacol* 2(4):458–462
- Saydam G, Aydin HH, Sahin F, Selvi N, Oktem G, Terzioğlu E, Buyukkececi F, Omay SB (2003) Involvement of protein phosphatase 2A in interferon-alpha-2b-induced apoptosis in K562 human chronic myelogenous leukaemia cells. *Leuk Res* 27(8):709–717
- Neviani P, Santhanam R, Trotta R, Notari M, Blaser BW, Liu S, Mao H, Chang JS, Galiotta A, Uttam A, Roy DC, Valtieri M, Bruner-Klisovic R, Caligiuri MA, Bloomfield CD, Marcucci G, Perrotti D (2005) The tumor suppressor PP2A is functionally inactivated in blast crisis CML through the inhibitory activity of the BCR/ABL-regulated SET protein. *Cancer Cell* 8:355–368
- Nobes CD, Lauritzen I, Mattei MG, Paris S, Hall A, Chardin P (1998) A new member of the Rho family, Rnd1, promotes disassembly of actin filament structures and loss of cell adhesion. *J Cell Biol* 141:187–197
- Kasof GM, Goyal L, White E (1999) Btf, a novel death-promoting transcriptional repressor that interacts with Bcl-2-related proteins. *Mol Cell Biol* 19:4390–4404
- Fritz G, Kaina B (2001) Ras-related GTPase RhoB represses NF-κB signaling. *J Biol Chem* 276:3115–3122
- Esteve P, Embade N, Perona R, Jimenez B, del Peso L, Leon J, Arends M, Miki T, Lacal JC (1998) Rho-regulated signals

- induce apoptosis in vitro and in vivo by a p53-independent, but Bcl2 dependent pathway. *Oncogene* 17:1855–1869
31. Embade N, Valeron PF, Aznar S, Lopez-Collazo E, Juan Carlos Lacal (2000) Apoptosis induced by Rac GTPase correlates with induction of FasL and ceramides production. *Mol Biol Cell* 11:4347–4358
 32. Lange T, Gunther C, Kohler T, Krahel R, Musiol S, Leiblein S, Al-Ali HK, van Hoomissen I, Niederwieser D, Deininger MW (2003) High levels of BAX, low levels of MRP-1, and high platelets are independent predictors of response to imatinib in myeloid blast crisis of CML. *Blood* 101(6):2152–2155
 33. La Rosee P, Johnson K, O'Dwyer ME, Druker BJ (2002) In vitro studies of the combination of imatinib mesylate (Gleevec) and arsenic trioxide (Trisenox) in chronic myelogenous leukemia. *Exp Hematol* 30(7):729–737
 34. Tarumoto T, Nagai T, Ohmine K, Miyoshi T, Nakamura M, Kondo T, Mitsugi K, Nakano S, Muroi K, Komatsu N, Ozawa K (2004) Ascorbic acid restores sensitivity to imatinib via suppression of Nrf2-dependent gene expression in the imatinib-resistant cell line. *Exp Hematol* 32(4):375–381